Contribution from the Lehrstuhl für Anorganische Chemie I, Ruhr-Universität, D-4630 Bochum, FRG, and Anorganisch-Chemisches Institut, Universität Heidelberg, D-6900 Heidelberg, FRG

Intramolecular, Base-Induced Formation of a Metal–Metal Bond in $[L_2Mo^{III}_2(\mu\text{-}OH)(\mu\text{-}CH_3CO_2)_2]^{3+}$ (L = 1,4,7-Trimethyl-1,4,7-triazacyclononane). Crystal Structures of $[L_2Mo^{III}_2(\mu\text{-}OH)(\mu\text{-}CH_3CO_2)_2](ClO_4)_3\cdot H_2O$ and $[L_2Mo^{III}_2(\mu\text{-}O)(\mu\text{-}CH_3CO_2)_2](ClO_4)(BF_4)\cdot H_2O$ and of the Mixed-Valence Complex $[L_2Mo^{III}Mo^{IV}(\mu\text{-}O)(\mu\text{-}CH_3CO_2)_2](ClO_4)_3\cdot H_2O$

Karl Wieghardt,*[1a] Ursula Bossek,[1a] Ademir Neves,[1a] Bernhard Nuber,[1b] and Johannes Weiss[1b]

Received June 22, 1988

Hydrolysis of $LMo^{III}Br_3$ (L = 1,4,7-trimethyl-1,4,7-triazacyclononane, $C_9H_{21}N_3$) in aqueous solution containing ammonium acetate under anaerobic conditions affords red $[L_2Mo_2(\mu\text{-}OH)(\mu\text{-}CH_3CO_2)_2]^{3+}$ (**1**): the PF_6 salt, $(1)(PF_6)_3$, has been isolated. The crystal structure of $(1)(ClO_4)_3\cdot H_2O$ has been determined by X-ray crystallography. Crystal data: orthorhombic; $P2_12_12_1$; a = 13.047 (7) Å, b = 15.769 (5) Å, c = 19.116 (9) Å, V = 3932.9 (8) Å^3, Z = 4. Two pseudooctahedral Mo^{III} centers are connected by a hydroxo group and two symmetrical acetato bridges. The Mo···Mo distance is 3.555 (1) Å, indicating the absence of a Mo···Mo bonding interaction. The complex is paramagnetic at ambient temperature (μ_{eff} = 2.9 μ_B/dimer). The μ-OH bridge in **1** may be deprotonated in aqueous solution (pK_a = 7.3 ± 0.2 at 25 °C) yielding the brown oxo-bridged species $[L_2Mo^{III}_2(\mu\text{-}O)(\mu\text{-}CH_3CO_2)_2]^{2+}$ (**2**). Crystal data for $(2)(BF_4)(ClO_4)\cdot H_2O$: triclinic; $P\bar{1}$; a = 12.263 (6) Å, b = 12.550 (5) Å, c = 13.258 (6) Å, α = 79.70 (3)°, β = 67.64 (3)°, γ = 66.56 (3)°; V = 1730.4 (6) Å^3, Z = 2. In diamagnetic **2** the Mo–Mo distance is only 2.885 (1) Å, indicating a bonding interaction. Thus deprotonation of **1** leads to the formation of a Mo–Mo bond. Electrochemically, **2** undergoes two reversible one-electron-transfer processes in acetonitrile to produce the mixed valence $Mo^{II}Mo^{III}$ species at $E_{1/2}$ = −2.31 V and a $Mo^{III}Mo^{IV}$ dimer at $E_{1/2}$ = −0.49 V vs Fc^+/Fc. The latter has been synthesized by air oxidation of **2** to yield blue-green $[L_2Mo^{III}Mo^{IV}(\mu\text{-}O)(\mu\text{-}CH_3CO_2)_2]^{3+}$ (**3**). Crystal data for $(3)(ClO_4)_3\cdot H_2O$: monoclinic; $C2/c$; a = 35.202 (5) Å, b = 10.674 (2) Å, c = 21.513 (5) Å, β = 113.97 (1)°; V = 7386.3 (12) Å^3, Z = 8. In **3** both Mo centers are equivalent; the Mo–Mo distance is 2.969 (1) Å. Magnetic susceptibility measurements indicate the presence of one unpaired electron per dimer.

Introduction

The possible mechanisms of the formation of metal–metal-bonded dimers prepared by starting from mononuclear precursor complexes in solution are virtually unknown. To illustrate this statement, consider the following well-known chemistry of molybdenum(III) complexes in aqueous solution. Hydrolysis of $[MoCl_6]^{3-}$ or $[MoCl_5(OH_2)]^{2-}$ in aqueous *p*-toluenesulfonic acid under anaerobic conditions yields the yellow, paramagnetic, monomeric hexaaquamolybdenum(III) trication.[2,3] The chemistry and structure[4] of this species, including the associative nature of its anation reactions[5] (and water-exchange process[6]), are well established and understood. On the other hand, the reduction of molybdate(VI) by zinc amalgam affords a diamagnetic, green, dimeric aqua ion of Mo(III), which has been formulated as $[(H_2O)_4Mo(\mu\text{-}OH)_2Mo(OH_2)_4]^{4+}$.[7] It has recently been shown by EXAFS spectroscopy that the Mo···Mo distance is short (2.54 Å), and consequently, a Mo≡Mo triple bond has been proposed.[8] But at which point during the reaction is the first direct Mo–Mo bonding interaction formed? It is astounding, at first glance, that even in 0.5 M solutions of $[Mo(OH_2)_6]^{3+}$ no dimer formation has been observed, and conversely, the dimer has not been reported to be readily cleaved to the monomer. Obviously, equilibrium 1

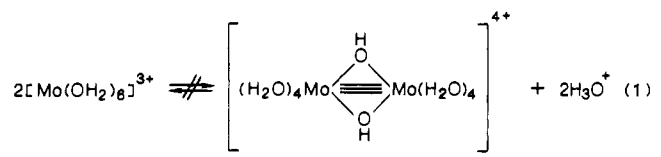

does not exist in aqueous solution, contrasting in this respect with $[Cr(OH_2)_6]^{3+}$, which forms dimers, trimers, and polymers via olation reactions.[9]

The reason for the nonexistence of (1) may be that two $[Mo(OH_2)_6]^{3+}$ species cannot come close enough in solution with concomitant loss of aqua ligands to allow an overlap of molybdenum d orbitals to form a metal–metal bond. Once this bond has formed via some unknown reaction path, it is not readily cleaved except via oxidative-addition reactions where electrons are removed from the Mo≡Mo triple bond.[10]

We here report the synthesis, electronic and magnetic properties, and crystal structure of $[L_2Mo^{III}_2(\mu\text{-}OH)(\mu\text{-}CH_3CO_2)_2](PF_6)_3$, $(1)(PF_6)_3$, a binuclear complex of molybdenum(III) containing a hydroxo bridge and two symmetrical acetato bridges (L = 1,4,7-trimethyl-1,4,7-triazacyclononane). The Mo···Mo distance of 3.555 (1) Å rules out an attractive metal–metal interaction between the two Mo(III) atoms. Upon deprotonation of **1** the (μ-oxo)bis(μ-acetato)dimolybdenum(III) species **2** forms. The crystal structure reveals that in **2** a Mo–Mo bonding interaction exists; the Mo–Mo bond distance is 2.885 (1) Å. Thus we have here a base-induced intramolecular formation of a metal–metal bond (eq 2). The process is reversible: protonation of **2** yields

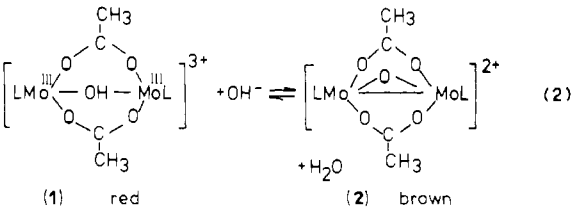

1. Some aspects of this work have already been communicated.[11]

In aprotic solvents **2** may be electrochemically reversibly reduced and oxidized by one electron, respectively (eq 3), generating the mixed-valence dimers $[Mo^{II}Mo^{III}]^+$ and $[Mo^{III}Mo^{IV}]^{3+}$. **3**

$$[L_2Mo^{II}Mo^{III}(\mu\text{-}O)(\mu\text{-}CH_3CO_2)_2]^+ \underset{-e^-}{\overset{+e^-}{\rightleftharpoons}} 2 \underset{+e^-}{\overset{-e^-}{\rightleftharpoons}} [L_2Mo^{III}Mo^{IV}(\mu\text{-}O)(\mu\text{-}CH_3CO_2)_2]^{3+} \quad (3)$$

(1) (a) Ruhr-Universität. (b) Universität Heidelberg.
(2) (a) Bowen, A. R.; Taube, H. *J. Am. Chem. Soc.* **1971**, *93*, 3287. (b) Kustin, K.; Toppen, D. *Inorg. Chem.* **1972**, *11*, 2851. (c) Bowen, A. R.; Taube, H. *Inorg. Chem.* **1974**, *13*, 2245.
(3) Sasaki, Y.; Sykes, A. G. *J. Chem. Soc., Chem. Commun.* **1973**, 767.
(4) Brorson, M.; Gajhede, M. *Inorg. Chem.* **1987**, *26*, 2109.
(5) (a) Sasaki, Y.; Sykes, A. H. *J. Chem. Soc., Dalton Trans.* **1975**, 1048. (b) Kelly, H. M.; Richens, D. T.; Sykes, A. G. *J. Chem. Soc., Dalton Trans.* **1984**, 2099.
(6) Richens, D. T.; Ducommun, Y.; Merbach, A. E. *J. Am. Chem. Soc.* **1987**, *109*, 603.
(7) Ardon, M.; Pernick, A. *Inorg. Chem.* **1974**, *9*, 2275.
(8) (a) Cramer, S. P.; Eiden, P. K.; Paffett, M. T.; Winkler, J. R.; Dori, Z.; Gray, H. B. *J. Am. Chem. Soc.* **1983**, *105*, 799. (b) Richens, D. T.; Helm, L.; Pittet, P.-A.; Merbach, A. E. *Inorg. Chim. Acta* **1987**, *132*, 85.
(9) Stünzi, H.; Marty, W. *Inorg. Chem.* **1983**, *22*, 2145.
(10) See for example the excellent review by: Chisholm, M. H. *Angew. Chem. Int., Ed. Engl.* **1986**, *25*, 21.
(11) Neves, A.; Bossek, U.; Wieghardt, K., Nuber, B.; Weiss, J. *Angew. Chem., Int. Ed. Engl.* **1988**, *27*, 685.

0020-1669/89/1328-0432$01.50/0

Table I. Crystallographic Data for the Complexes

	$(1)(ClO_4)_3 \cdot H_2O$	$(2)(ClO_4)(BF_4) \cdot H_2O$	$(3)(ClO_4)_3 \cdot H_2O$
formula	$[C_{22}H_{49}Mo_2N_6O_5](ClO_4)_3 \cdot H_2O$	$[C_{22}H_{48}Mo_2N_6O_5](BF_4)(ClO_4) \cdot H_2O$	$[C_{22}H_{48}Mo_2N_6O_5](ClO_4)_3 \cdot H_2O$
fw	985.90	872.8	984.90
space group	$P2_12_12_1$	$P\bar{1}$	$C2/c$
a, Å	13.047 (7)	12.263 (6)	35.202 (5)
b, Å	15.769 (5)	12.550 (5)	10.674 (2)
c, Å	19.116 (9)	13.258 (6)	21.513 (5)
α, deg		79.70 (3)	
β, deg		67.64 (3)	113.97 (1)
γ, deg		66.56 (3)	
V, Å^3	3932.9 (8)	1730.4 (6)	7386.3 (12)
Z	4	2	8
ρ_{calcd}, g cm^{-3}	1.66	1.69	1.75
transmissn coeff T_{max}/T_{min}	1.0–0.90	1.0–0.82	1.0–0.73
R	0.057	0.058	0.064
R_w	0.056	0.052	0.058

has been isolated and characterized by X-ray crystallography; the Mo–Mo distance in **3** is 2.969 (1) Å.

Experimental Section

The ligand 1,4,7-trimethyl-1,4,7-triazacyclononane (L)[12] and $LMoBr_3$[13] have been prepared according to procedures described in the literature.

Caution! The perchlorate salts of all molybdenum dimers described in this paper were found to be shock and heat sensitive; they explode uncontrollably and violently and should not be prepared in amounts larger than 20 mg. We have used these salts for X-ray crystallography only because the ClO_4 salts gave suitable single crystals for X-ray crystallographic investigations whereas the PF_6 salts did not.

Synthesis of Complexes. $[L_2Mo_2(\mu\text{-}OH)(\mu\text{-}CH_3CO_2)_2](PF_6)_3$, $(1)(PF_6)_3$. To a deoxygenated aqueous solution (40 mL) of ammonium acetate (2.4 g; 32 mmol) was added $LMoBr_3$ (0.70 g, 1.4 mmol) under an argon atmosphere at room temperature with stirring. The suspension was refluxed for 4 h until a clear red-brown solution was obtained. Addition of $NaPF_6$ (0.5 g) at 20 °C to this solution initiated the precipitation of red microcrystalline $(1)(PF_6)_3$. After this mixture was allowed to stand for 24 h at 0 °C, these crystals were filtered off and recrystallized from a minimum amount of water by addition of solid $NaPF_6$. Yield: 0.8 g. IR (KBr; cm^{-1}): ν(OH) 3570 (m); ν_{as}(CO) 1560 (vs); ν_s(CO) 1460, 1475 (vs).

Anal. Calcd for $[C_{22}H_{49}Mo_2N_6O_5](PF_6)_3$: C, 23.93; H, 4.47; N, 7.61. Found: C, 24.1; H, 4.45; N, 7.6.

From an aqueous solution of $(1)(PF_6)_3$ at 50 °C the corresponding salt $(1)(ClO_4)_3 \cdot H_2O$ was obtained by addition of solid $NaClO_4$ and slow cooling to room temperature (1 °C/h) as single crystals suitable for X-ray crystallography. *Caution!* This ClO_4 salt exploded violently upon crunching of crystals with a metal spatula.

$[L_2Mo^{III}_2(\mu\text{-}O)(\mu\text{-}CH_3CO_2)_2](PF_6)_2 \cdot 3H_2O$, $(2)(PF_6)_2 \cdot 3H_2O$. To an argon-purged aqueous solution (30 mL) of $(1)(PF_6)_3$ (0.10 g, 0.09 mmol) was added triethylamine (1 mL) at room temperature. The original red color changed to deep brown. Addition of solid $NaPF_6$ (0.5 g) initiated the immediate precipitation of brown microcrystals of $(2)(PF_6)_2 \cdot 3H_2O$. Yield: 0.07 g. IR (KBr; cm^{-1}): ν_{as}(C–O) 1510 (vs); ν_s(C–O) 1460, 1425 (ms). Anal. Calcd for $[C_{22}H_{48}Mo_2N_6O_5](PF_6)_2 \cdot 3H_2O$: C, 26.10; H, 5.38; N, 8.30. Found: C, 26.0; H, 5.2; N, 8.2.

Single crystals for X-ray crystallography of $(2)(BF_4)(ClO_4) \cdot 2H_2O$ were grown from an aqueous solution of $(2)(PF_6)_2 \cdot 3H_2O$ to which triethylamine and solid $NaClO_4$ were added. The brown $(2)(ClO_4)_2$ was rapidly filtered off, but *not* dried; it was immediately redissolved in water containing $N(C_2H_5)_3$. Then solid $NaBF_4$ was added at 40 °C. Slow cooling of this solution to 0 °C (1 °C/h) afforded brown single crystals suitable for X-ray crystallography of $(2)(BF_4)(ClO_4) \cdot H_2O$. *Caution!* This salt and the pure ClO_4 salt are very explosive if crushed with a metal spatula or heated.

$[L_2Mo^{III}Mo^{IV}(\mu\text{-}O)(\mu\text{-}CH_3CO_2)_2](PF_6)_3$, $(3)(PF_6)_3$. Method A. Wet $(1)(ClO_4)_3 \cdot H_2O$ (0.2 g, 0.2 mmol) was dissolved in a mixture of concentrated $HClO_4$ (70–72%) (15 mL) and water (5 mL) at room temperature. This solution was allowed to stand at room temperature in an open vessel in the presence of air for 12 h. The original red color changed to bluish green. Addition of $NaClO_4$ (0.5 g) dissolved in water (5 mL) initiated the precipitation of bluish green crystals of $(3)(ClO_4)_3 \cdot H_2O$, which were filtered off, and were immediately redissolved in water. Upon addition of $NaPF_6$ (0.5 g) bluish green crystals of $(3)(PF_6)_3$ precipitated. Yield: 0.2 g. Probably due to hydrolysis reactions of PF_6^- in acidic aqueous solution the above synthesis is not feasible in a ClO_4-free, PF_6-containing medium. Dry crystals of $(3)(ClO_4)_3 \cdot H_2O$ are again explosive. IR (KBr, cm^{-1}): ν_{as}(C–O) 1560 (vs); ν_s(C–O) 1470, 1450 (vs). Anal. Calcd for $[C_{22}H_{48}Mo_2N_6O_5](PF_6)_3$: C, 23.95; H, 4.38; N, 7.62. Found: C, 24.0; H, 4.4; N, 7.5.

Method B. Single crystals suitable for X-ray crystallography of $(3)(ClO_4)_3 \cdot H_2O$ were obtained from an acetonitrile solution (30 mL) of $(1)(ClO_4)_3 \cdot H_2O$ (0.1 g) to which $NaClO_4$ (0.1 g) was added. This solution was allowed to stand in an open vessel in the presence of air for 24 h. Single crystals of $(3)(ClO_4)_3 \cdot H_2O$ grew slowly.

Electrochemistry. Electrochemical experiments were performed with a Princeton Applied research (PAR) Model 173 potentiostat, a PAR Model 175 universal programmer, a Model 179 digital coulometer, and a Kipp & Zonen X-Y recorder. Cyclic voltammograms (CV) were made on acetonitrile solutions containing 0.1 M tetra-*n*-butylammonium hexafluorophosphate ($(TBA)PF_6$) as supporting electrolyte, and were conducted at 22 °C under an argon atmosphere. A standard three-electrode system was used, comprising a glassy-carbon working electrode, a platinum-wire auxiliary electrode and an Ag/AgCl (saturated LiCl in ethanol) reference electrode. The performance of the reference electrode was monitored by measuring the Fe (+1/0) couple) of ferrocene (+0.537 V vs Ag/AgCl).[14] CVs were measured in aqueous buffer solutions at an Au working electrode. The pH dependence was measured by using a glycine/NaOH/NaCl, boric acid/KCl/NaOH, borax/HCl, KH_2PO_4/Na_2HPO_4, citric acid/NaOH, or a sodium acetate/acetic acid buffer. Diagnostic criteria for the reversibility of electron-transfer processes were employed in the usual manner.[15] Scan rates of CVs were between 20 and 200 mV s^{-1}.

Magnetic Measurements. Magnetic susceptibilities of powdered samples were recorded on a Faraday-type magnetometer using a sensitive Cahn RG electrobalance in the temperature range 4.2–289.5 K. Details of the apparatus have been described elsewhere.[16] Experimental susceptibility data were corrected for the underlying diamagnetism. These corrections for diamagnetism were estimated as -551×10^{-6} cm^3/mol of dimer of $(1)(PF_6)_3$ and -468×10^{-6} cm^3/mol of dimer of $(3)(ClO_4)_3 \cdot H_2O$. No corrections for temperature-independent paramagnetism were applied.

Instrumentation. Electronic absorption spectra in the 200–1200-nm range were recorded with a Perkin-Elmer Lambda 9 spectrophotometer, while the infrared spectra (KBr disks) were recorded with a Perkin-Elmer Model 283 B spectrophotometer.

X-ray Crystallography. A red column-shaped crystal of **1**, a brown irregular crystal of **2**, and a tabular-shaped bluish green crystal of **3** were attached to glass fibers and mounted on a four-circle diffractometer. The unit cell dimensions were obtained by a least-squares fit of 27 reflections ($4 < 2\theta < 23°$), respectively. The data are summarized for **1–3** in Table I. Intensity data were corrected for Lorentz and polarization effects; empirical absorption corrections (ψ-scans of seven reflections; $5 < 2\theta < 40°$ for each crystal) were also carried out.[17] The function minimized during least-squares refinements was $\sum w(|F_o| - |F_c|)^2$. The structures were solved via conventional Patterson and Fourier syntheses. Neutral-atom scattering factors and anomalous dispersion corrections for

(12) Wieghardt, K.; Chaudhuri, P.; Nuber, B.; Weiss, J. *Inorg. Chem.* **1982**, *21*, 3086.
(13) Backes-Dahmann, G.; Herrmann, W.; Wieghardt, K.; Weiss, J. *Inorg. Chem.* **1985**, *24*, 485.
(14) (a) Gagné, R. R.; Koval, C. A.; Lisensky, G. C. *Inorg. Chem.* **1980**, *19*, 2854. (b) Gritzner, G.; Kuta, J. *Pure Appl. Chem.* **1982**, *54*, 1527.
(15) Nicholson, R. S.; Shain, I. *Anal. Chem.* **1964**, *36*, 706.
(16) Merz, L.; Haase, W. *J. Chem. Soc., Dalton Trans.* **1980**, 875.
(17) All computations were carried out on an ECLIPSE computer using the SHELXTL program package.

Table II. Atom Coordinates ($\times 10^4$) and Temperature Factors ($Å^2 \times 10^3$) for $(1)(ClO_4)_3 \cdot H_2O$

atom	x	y	z	U_{eq}[a]
Mo(1)	1536 (1)	4507 (1)	6663 (1)	28 (1)*
N(1)	5457 (7)	10689 (6)	4206 (4)	38 (3)*
N(2)	5086 (6)	10310 (6)	2764 (4)	36 (3)*
N(3)	6127 (7)	11820 (6)	3136 (5)	43 (3)*
C(1)	4560 (9)	10140 (9)	4002 (6)	53 (4)*
C(2)	4204 (8)	10298 (7)	3264 (7)	50 (4)*
C(3)	5016 (10)	11062 (7)	2293 (6)	45 (4)*
C(4)	5224 (10)	11890 (8)	2681 (7)	54 (5)*
C(5)	5901 (11)	12155 (7)	3871 (6)	51 (4)*
C(6)	5184 (11)	11617 (8)	4264 (7)	58 (5)*
C(7)	5826 (10)	10382 (9)	4881 (6)	55 (4)*
C(8)	5064 (9)	9507 (7)	2352 (6)	47 (4)*
C(9)	7024 (11)	12327 (8)	2839 (7)	57 (5)*
Mo(2)	9119 (1)	9905 (1)	3673 (1)	30 (1)*
N(4)	9687 (7)	9847 (6)	4743 (4)	43 (3)*
N(5)	10402 (7)	9026 (7)	3527 (5)	49 (4)*
N(6)	10381 (7)	10839 (6)	3593 (5)	41 (3)*
C(11)	10508 (10)	9168 (9)	4819 (7)	57 (5)*
C(12)	10470 (10)	8578 (7)	4219 (7)	53 (5)*
C(13)	11383 (8)	9550 (9)	3364 (8)	62 (5)*
C(14)	11128 (8)	10415 (8)	3115 (7)	51 (4)*
C(15)	10770 (9)	11047 (8)	4327 (6)	52 (4)*
C(16)	10111 (10)	10742 (8)	4871 (6)	51 (4)*
C(17)	8851 (9)	9686 (9)	5255 (6)	55 (5)*
C(18)	10215 (11)	8393 (8)	2943 (8)	61 (5)*
C(19)	10106 (11)	11646 (8)	3248 (7)	56 (5)*
O(1)	6615 (5)	9188 (4)	3551 (4)	42 (2)*
O(2)	8202 (6)	8823 (5)	3771 (5)	49 (3)*
O(3)	7301 (5)	10411 (5)	2384 (4)	40 (2)*
O(4)	8907 (5)	10016 (5)	2601 (4)	44 (3)*
O(5)	7898 (5)	10741 (4)	3883 (4)	35 (2)*
C(20)	7238 (7)	8654 (7)	3721 (7)	41 (4)*
C(21)	6973 (11)	7746 (8)	3793 (9)	75 (6)*
C(22)	8207 (9)	10253 (7)	2200 (6)	41 (4)*
C(23)	8434 (10)	10366 (9)	1447 (5)	61 (5)*
Cl(1)	6471 (3)	2798 (2)	798 (2)	62 (1)*
O(11)	6283 (12)	3315 (10)	1365 (8)	148 (6)
O(12)	7262 (12)	2149 (10)	966 (8)	136 (5)
O(13)	5705 (18)	2501 (16)	420 (11)	248 (11)
O(14)	6937 (17)	3340 (14)	314 (11)	216 (9)
Cl(2)	7362 (2)	7965 (2)	1425 (2)	53 (1)*
O(21)	6449 (10)	8335 (8)	1189 (6)	101 (4)
O(22)	7237 (10)	7114 (8)	1586 (7)	108 (4)
O(23)	8111 (13)	8036 (10)	924 (8)	155 (6)
O(24)	7718 (15)	8341 (12)	1995 (9)	177 (7)
Cl(3)	2091 (3)	9476 (3)	1086 (2)	80 (1)*
O(31)	2790 (21)	9317 (17)	1509 (14)	288 (12)
O(32)	2267 (18)	9603 (15)	424 (12)	247 (11)
O(33)	1300 (20)	10040 (16)	1239 (12)	245 (11)
O(34)	1391 (22)	8790 (17)	1073 (13)	270 (12)
W(1)	1681 (8)	7249 (6)	403 (5)	76 (4)*

[a] An asterisk denotes the equivalent isotropic U defined as one-third of the trace of the orthogonalized U_{ij} tensor.

Table III. Atom Coordinates ($\times 10^4$) and Temperature Factors ($Å^2 \times 10^3$) for $(2)(BF_4)(ClO_4) \cdot H_2O$

atom	x	y	z	U_{eq}[a]
Mo(1)	1841 (1)	2476 (1)	1930 (1)	29 (1)*
Mo(2)	9262 (1)	2598 (1)	2627 (1)	28 (1)*
O(1)	643 (3)	2015 (4)	3203 (3)	47 (2)*
O(2)	1982 (3)	1549 (3)	685 (3)	41 (2)*
C(20)	1095 (5)	1528 (5)	460 (4)	36 (2)*
C(21)	1382 (6)	898 (6)	−518 (5)	56 (3)*
O(3)	−43 (3)	2003 (3)	1039 (3)	43 (2)*
O(4)	994 (4)	4136 (3)	1316 (3)	48 (2)*
C(22)	−171 (5)	4753 (5)	1617 (4)	37 (3)*
C(23)	−561 (6)	5999 (5)	1262 (5)	53 (3)*
O(5)	−1007 (3)	4342 (3)	2197 (3)	44 (2)*
N(1)	3353 (4)	948 (4)	2393 (4)	42 (2)*
N(2)	3666 (4)	2718 (4)	756 (4)	42 (2)*
N(3)	2308 (4)	3325 (4)	2981 (4)	49 (3)*
C(1)	4583 (6)	769 (6)	1504 (7)	100 (4)*
C(2)	4694 (6)	1582 (6)	689 (5)	82 (4)*
C(3)	3878 (8)	3577 (8)	1210 (7)	109 (6)*
C(4)	3191 (8)	3906 (8)	2249 (6)	97 (6)*
C(5)	2953 (9)	2400 (7)	3633 (6)	106 (6)*
C(6)	3358 (9)	1243 (7)	3411 (7)	110 (6)*
C(7)	3107 (6)	−136 (5)	2583 (6)	65 (4)*
C(8)	3629 (6)	3094 (7)	−353 (5)	77 (4)*
C(9)	1201 (7)	4184 (7)	3707 (7)	95 (5)*
N(4)	−2667 (4)	3023 (4)	2460 (4)	46 (2)*
N(5)	−2075 (4)	3083 (4)	4337 (3)	40 (2)*
N(6)	−1131 (4)	947 (4)	3259 (4)	39 (2)*
C(11)	−3687 (6)	3604 (8)	3440 (6)	107 (5)*
C(12)	−3301 (6)	3854 (7)	4222 (6)	75 (4)*
C(13)	−2163 (7)	1983 (6)	4980 (5)	75 (4)*
C(14)	−1410 (8)	938 (6)	4438 (5)	80 (4)*
C(15)	−2217 (7)	938 (6)	3021 (7)	77 (4)*
C(16)	−2687 (8)	1882 (7)	2334 (7)	88 (5)*
C(17)	−2805 (7)	3757 (7)	1483 (5)	72 (4)*
C(18)	−1714 (6)	3717 (7)	4916 (5)	68 (4)*
C(19)	−15 (6)	−114 (5)	2832 (6)	72 (4)*
Cl(1)	6161 (3)	7807 (3)	3734 (2)	83 (2)*
O(11)	5148 (5)	8369 (6)	4555 (5)	119 (4)*
O(12)	5919 (9)	7633 (12)	2961 (7)	328 (10)*
O(13)	6887 (9)	6852 (6)	4006 (6)	195 (7)*
O(14)	6807 (11)	8381 (10)	3373 (9)	330 (11)*
Cl(2)	2455 (3)	7276 (3)	1387 (3)	65 (2)*
O(21)	3469 (5)	6374 (4)	846 (5)	103 (3)*
O(22)	1444 (6)	7039 (6)	1690 (7)	172 (5)*
O(23)	2372 (7)	8231 (6)	698 (6)	159 (5)*
O(24)	2569 (7)	7593 (6)	2211 (6)	150 (5)*
W(1)	9440 (11)	7253 (10)	3757 (9)	105 (4)
W(2)	4632 (15)	6161 (14)	2977 (12)	163 (6)

[a] An asterisk denotes the equivalent isotropic U defined as one-third of the trace of the orthogonalized U_{ij} tensor.

non-hydrogen atoms were taken from ref 18 and hydrogen atom scattering factors from ref 19. The positions of methyl (rigid body refinement) and methylene protons were calculated (d(C–H) = 0.96 Å, sp^3 carbon) and were included in the final refinement cycle with isotropic thermal parameters. All non-hydrogen atoms were refined with use of anisotropic displacement parameters with the exception of the oxygen atoms of the perchlorate anions for which isotropic thermal parameters were used. In **2** and **3** some degree of disorder of the ClO_4 and BF_4 ions was observed. In **2** the BF_4 and ClO_4 ions are statistically distributed over two crystallography independent positions at a ratio of 1:1, which was determined by treating the occupancy factors of these two Cl/B positions as variables. A best fit was obtained with an occupancy of 0.55 for B and 0.45 for Cl, which was set at 0.5 for both atoms in the final refinement cycle. The F and O atoms are crystallographically indistinguishable since the bond distances B–F and Cl–O are very similar. In addition, the water molecule of crystallization per formula unit of **2** occupies two independent positions with an occupancy factor of 0.5, respectively. In **3** the ClO_4 anions (Cl(1), Cl(3), and Cl(4)) are also disordered.

In the final refinement cycle the ratios between maximum and mean shift/esd were as follows: **1**, 0.72/0.14; **2**, 0.65/0.16; **3**, 1.4/0.14. The highest peaks in the final difference Fourier map were as follows: **1**, 1.4 e/Å^3; **2**, 0.95 e/Å^3; **3**, 1.07 e/Å^3, all of which are in the neighborhood of disordered ClO_4 or BF_4 ions. Final atom parameters for **1–3** are listed in Tables II–IV, respectively. An enantiomorph determination of **1** has been carried out that proved the choice reported here to be correct.

Results and Discussion

Preparation of Complexes. Complexes containing the (μ-oxo)- or (μ-hydroxo)bis(μ-acetato)dimetal(III) core have been prepared from monomeric octahedral compounds LMX_3, where L represents a facially capping nitrogen donor ligand such as 1,4,7-triazacyclononane, its N-trimethylated derivative, or hydrotris(pyrazolyl)borate(1−), X is Cl or Br and M is iron(III),[20,21] manga-

(18) *International Tables for X-ray Crystallography*, Kynoch: Birmingham, England, 1974; Vol. IV, pp 99, 149.
(19) Stewart, R. F.; Davidson, E. R.; Simpson, W. T. *J. Chem. Phys.* **1965**, *42*, 3175.
(20) (a) Armstrong, W. H.; Lippard, S. J. *J. Am. Chem. Soc.* **1983**, *105*, 4837. (b) Armstrong, W. H.; Spool, A.; Papaefthymiou, G. C.; Frankel, R. B.; Lippard, S. J. *J. Am. Chem. Soc.* **1984**, *106*, 3653.
(21) Wieghardt, K.; Pohl, K.; Gebert, W. *Angew. Chem., Int. Ed. Engl.* **1983**, *22*, 727.

Table IV. Atom Coordinates (×10⁴) and Temperature Factors (Å² × 10³) for $(3)(ClO_4)_3 \cdot H_2O$

atom	x	y	z	U_{eq}[a]
Mo(1)	1126 (1)	6938 (1)	1619 (1)	39 (1)*
N(1)	710 (2)	7917 (8)	2007 (4)	48 (4)*
N(2)	1533 (2)	7062 (8)	2708 (4)	43 (3)*
N(3)	883 (2)	5324 (8)	2047 (4)	41 (4)*
C(1)	1002 (3)	8660 (11)	2596 (5)	64 (6)*
C(2)	1347 (3)	7884 (11)	3075 (5)	61 (5)*
C(3)	1574 (3)	5752 (10)	2972 (5)	53 (5)*
C(4)	1161 (3)	5124 (11)	2779 (5)	63 (5)*
C(5)	460 (3)	5740 (11)	1948 (5)	57 (5)*
C(6)	470 (3)	7039 (11)	2248 (5)	58 (5)*
C(7)	411 (3)	8797 (11)	1498 (5)	59 (5)*
C(8)	1959 (3)	7514 (11)	2839 (5)	55 (5)*
C(9)	861 (3)	4138 (10)	1689 (5)	57 (5)*
Mo(2)	1380 (1)	8086 (1)	589 (1)	41 (1)*
N(4)	1515 (3)	8046 (8)	−340 (4)	55 (4)*
N(5)	1105 (3)	9887 (9)	101 (4)	56 (4)*
N(6)	1941 (3)	9257 (8)	914 (4)	46 (4)*
C(11)	1211 (4)	8818 (13)	−841 (6)	90 (7)*
C(12)	1095 (4)	9963 (12)	−600 (6)	95 (8)*
C(13)	1396 (4)	10841 (13)	535 (8)	123 (9)*
C(14)	1816 (4)	10569 (11)	797 (7)	80 (7)*
C(15)	2175 (4)	8885 (13)	515 (7)	90 (8)*
C(16)	1939 (4)	8580 (14)	−162 (6)	94 (8)*
C(17)	1496 (6)	6759 (13)	−609 (8)	123 (11)*
C(18)	689 (5)	10094 (16)	60 (9)	128 (11)*
C(19)	2213 (4)	9061 (14)	1652 (6)	93 (7)*
O(1)	1518 (2)	5587 (6)	1541 (3)	40 (3)*
O(2)	1740 (2)	6501 (6)	833 (3)	46 (3)*
C(21)	1728 (3)	5576 (9)	1183 (5)	40 (4)*
C(22)	1975 (4)	4443 (10)	1197 (7)	69 (6)*
O(3)	622 (2)	6485 (6)	744 (3)	35 (3)*
O(4)	829 (2)	7275 (7)	−24 (3)	53 (3)*
C(23)	556 (3)	6788 (10)	137 (5)	42 (4)*
C(24)	134 (3)	6574 (11)	−412 (5)	54 (5)*
O(5)	1228 (2)	8539 (6)	1331 (3)	58 (3)*
Cl(1)	751 (1)	6247 (3)	4311 (2)	54 (1)*
O(11)	590 (3)	5315 (8)	3813 (4)	80 (3)
O(12)	587 (6)	7357 (19)	3985 (10)	105 (7)
O(13)	1117 (4)	6671 (13)	4357 (7)	172 (5)
O(14)	696 (6)	6023 (19)	4900 (11)	116 (7)
Cl(2)	3132 (1)	6645 (3)	2242 (2)	74 (2)*
O(21)	1844 (4)	12801 (12)	3076 (6)	157 (5)
O(22)	2211 (4)	11525 (12)	2615 (6)	159 (5)
O(23)	1514 (4)	11212 (13)	2199 (7)	187 (6)
O(24)	3088 (4)	5783 (15)	1770 (7)	199 (6)
Cl(3)	2500	2500	0	72 (2)*
O(31)	2369 (6)	12422 (16)	506 (10)	92 (5)
O(32)	2728 (7)	13466 (21)	437 (11)	128 (8)
O(33)	2945 (7)	2495 (21)	208 (11)	132 (8)
O(34)	2679 (8)	1405 (23)	406 (12)	144 (9)
Cl(4)	0	1565 (6)	2500	102 (3)*
O(41)	−249 (6)	467 (20)	2102 (11)	115 (7)
O(15)	417 (6)	6824 (19)	4387 (10)	109 (6)
O(16)	985 (6)	5675 (19)	4962 (10)	109 (7)
O(42)	340 (9)	2040 (30)	2469 (21)	437 (18)
O(43)	−73 (12)	1720 (31)	1836 (16)	567 (24)

[a] An asterisk denotes the equivalent isotropic U defined as one-third of the trace of the orthogonalized U_{ij} tensor.

nese(III),[22] or vanadium(III)[23] via hydrolysis in aqueous acetate containing media.

Walton and co-workers have described such a complex of osmium(IV), $Os^{IV}_2(\mu\text{-}O)(\mu\text{-}CH_3CO_2)_2X_4(PR_3)_2$,[24] and its mixed-valence $Os^{III}Os^{IV}$ analogue.

Hydrolysis of $LMoBr_3$[13] (L = 1,4,7-trimethyl-1,4,7-triazacyclononane) in an aqueous solution containing ammonium acetate

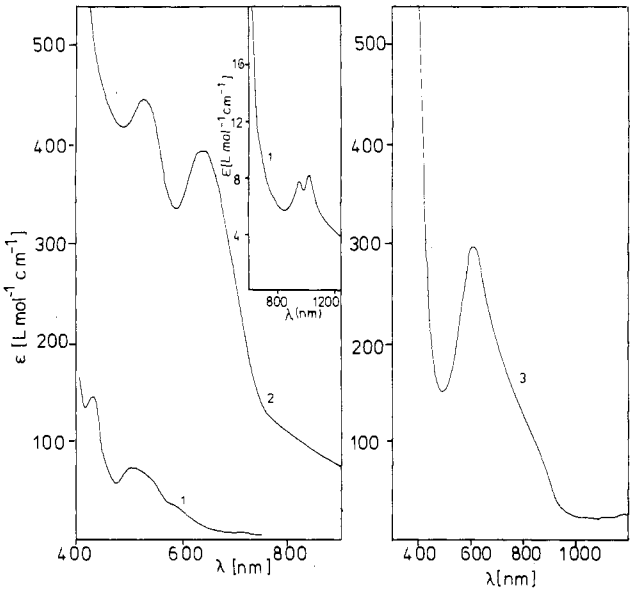

Figure 1. Electronic spectra of $(1)(PF_6)_3$, $(2)(PF_6)_2 \cdot 3H_2O$, and $(3)(ClO_4)_3 \cdot H_2O$ in acetonitrile at 20 °C.

under anaerobic conditions affords a red-brown solution from which upon addition of solid $NaPF_6$ red crystals of $(1)(PF_6)_3$ precipitated. **1** contains a (μ-hydroxo)bis(μ-acetato)dimolybdenum(III) core. In the solid state, salts are indefinitely stable toward oxygen, but in solution (acetonitrile or concentrated perchloric acid), the reaction with oxygen produces a bluish green compound (**3**), which was isolated as $(3)(PF_6)_3$ or $(3)(ClO_4)_3 \cdot H_2O$ (*Caution*! explosive). **3** is a $Mo^{III}Mo^{IV}$ mixed-valence species with a (μ-oxo)bis(μ-acetato)dimolybdenum(III/IV) core.

In alkaline aqueous solution **1** is deprotonated at the μ-OH bridge and the brown μ-oxo-bridged species (**2**) is formed. Reacidification yields quantitatively **1**. Thus equilibrium 2 exists in aqueous solution. Addition of $NaPF_6$ to such an alkaline solution affords brown microcrystals of $(2)(PF_6)_2 \cdot 3H_2O$.

The acid dissociation constant, K_a, of equilibrium 2 has been determined spectrophotometrically. At 25 °C a pK_a value of 7.3 ± 0.2 has been evaluated by using a variety of different buffer solutions (I = 0.1 M) in the pH range 1.3–11. The absorbance (Figure 1) at two different wavelengths (642 and 527 nm), where the fully protonated and fully deprotonated forms exhibit a large difference of absorbance, was monitored as function of pH. From the pH dependence of the cyclic voltammogram of **1** in aqueous solution, a value of 7.8 ± 0.3 at 20 °C and ionic strength 0.01 M has been found in reasonable agreement with the spectrophotometric determination (see below).

μ-Hydroxo bridges between two molybdenum(III) centers are known to be relatively acidic and the above pK_a value is not without precedence. For $[Mo_2(\mu\text{-}OH)_2(\mu\text{-}CH_3CO_2)(edta)]^-$ a pK_a value of 7.73 at 0 °C has been determined[25] (edta = ethylenediaminetetraacetate); the monodeprotonated form is the (μ-oxo)(μ-hydroxo)(μ-acetato)dimolybdenum(III) species.

Electronic Spectra and Magnetic Properties of Complexes. Figure 1 shows the electronic spectra of $(1)(PF_6)_3$, $(2)(PF_6)_2 \cdot 3H_2O$, and $(3)(ClO_4)_3 \cdot H_2O$ in acetonitrile at 20 °C, and Table V summarizes electronic spectra and magnetic properties of the complexes.

In the electronic spectrum of **1**, two bands of low intensity are observed at 501 and 431 nm that may tentatively be assigned as d–d transitions of the molybdenum(III) ions ($^4A_2 \rightarrow {}^4T_1$ and $^4A_2 \rightarrow {}^4T_2$, respectively) in a distorted octahedral N_3O_3 ligand field.[26] The molar absorption coefficients (per molybdenum (III)) are of the same order of magnitude as those reported for $Mo(OH_2)_6^{3+}$;[27] the distortion caused by the coordinated cyclic triamine

(22) Wieghardt, K.; Bossek, U.; Ventur, D.; Weiss, J. *J. Chem. Soc., Chem. Commun.* **1985**, 347.
(23) (a) Wieghardt, K.; Köppen, M.; Nuber, B.; Weiss, J. *J. Chem. Soc., Chem. Commun.* **1986**, 1530. (b) Köppen, M.; Fresen, G.; Wieghardt, K.; Llusar, R., Nuber, B.; Weiss, J. *Inorg. Chem.* **1988**, *27*, 721.
(24) Armstrong, J. E.; Robinson, W. R.; Walton, R. A. *Inorg. Chem.* **1983**, *22*, 1301.
(25) Shibahara, T.; Sykes, A. G. *J. Chem. Soc., Dalton Trans.* **1978**, 95.
(26) Lever, A. B. P. *Inorganic Electronic Spectroscopy*, 2nd ed.; Elsevier, 1984; pp 414 and 614.

Table V. Electronic Spectral Data and Magnetic Properties of Complexes

complex	electronic spectral data:[a] λ_{max}, nm (ϵ,[b] L mol^{-1} cm^{-1})	magnetism
(**1**)$(PF_6)_3$	1029 (8.6), 950 (8.3), 501 (66), 431 (120)	antiferromagnetic coupling; $J = -96$ cm^{-1}
(**2**)$(PF_6)_2 \cdot 3H_2O$	1000 (sh), 800 (sh), 644 (327), 527 (433)	diamagnetic
(**3**)$(PF_6)_3$	800 (sh), 605 (300)	μ_{eff}(50 K) = 1.6 μ_B/dimer; μ_{eff}(290 K) = 2.1 μ_B/dimer

[a] Measured in acetonitrile. [b] Absorption coefficients are per dimer.

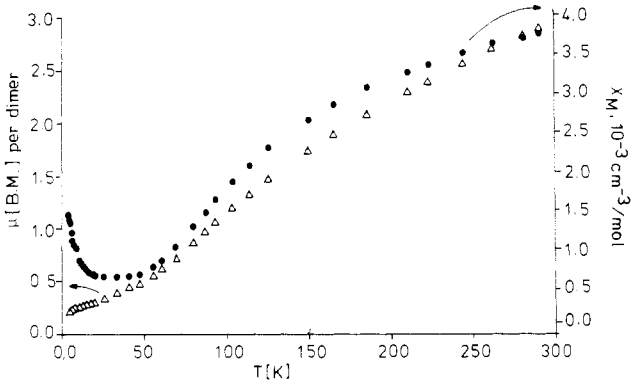

Figure 2. Magnetic susceptibility of (**1**)$(PF_6)_3$ as a function of the temperature (●: experimental data) and temperature dependence of the effective magnetic moment of (**1**)$(PF_6)_3$ (△: experimental data).

gives rise to a relative increase of intensity in **1** (factor of 2–4). Interestingly, at 1029 and 950 nm two further weak absorptions are observed that are assigned as spin-forbidden transitions. Thus the electronic spectrum of **1** is typical for octahedral Mo(III) (d^3) complexes with σ-donor ligands of the classical Werner type in agreement with the X-ray structure determination (see below).

Upon deprotonation of **1** the electronic spectrum changes dramatically. Two intense absorptions at 644 and 527 nm are observed for **2** that are believed to be associated with transitions arising from the Mo–Mo multiple bond in **2**. The mixed-valence species **3** exhibits one intense absorption in the visible at 605 nm.

Measurements of the magnetic susceptibility were carried out on solid samples of (**1**)$(PF_6)_3$, (**2**)$(PF_6)_2 \cdot 3H_2O$, and (**3**)$(ClO_4)_3 \cdot H_2O$ in the temperature range 4.2–289.5 K by use of the Faraday method. (**2**)$(PF_6)_2 \cdot 3H_2O$ and its perchlorate salt are diamagnetic. Plots of the molar susceptibility and effective moment versus temperature are given in Figure 2 for (**1**)$(PF_6)_3$.

For this complex, the temperature-dependent susceptibility could not be modeled satisfactorily by using the simple theory of Heisenberg, Dirac, and Van Vleck for magnetic coupling in a binuclear system ($S_1 = S_2 = {}^3/_2$). There are examples in the literature where similar magnetic data have been interpreted as arising from thermal population of excited states.[40] A complete analysis of the magnetic data of **2** will be published elsewhere. For the present purpose it may suffice to say that, clearly, an intramolecular antiferromagnetic coupling of the Mo(III) centers is observed with an $S = 0$ ground state (at very low temperatures a monomeric Mo(III) impurity prevails). Antiferromagnetic coupling has also been observed in the Cr^{III}_2 analogue $[L_2Cr_2(\mu\text{-}OH)(\mu\text{-}CH_3CO_2)_2](ClO_4)_3$[29] ($J = -15.5$ cm^{-1}). In the cofacial bioctahedral complexes $[X_3Mo(\mu\text{-}X)_3MoX_3]^{3+}$ (X = Cl, Br) antiferromagnetic coupling has also been observed,[30] but in contrast to **1**, a Mo–Mo bonding interaction has been proposed.

Figure 3 shows the molar magnetic susceptibility and the effective magnetic moment per dimer versus the temperature for (**3**)$(ClO_4)_3 \cdot H_2O$. In the temperature range 30–100 K, μ_{eff} does not vary much with the temperature and an effective magnetic moment of 1.65 μ_B/dimer indicates an $S = {}^1/_2$ ground state. Using an isotropic spin-exchange Hamiltonian, $H = -2JS_1 \cdot S_2$ with $S_1 = {}^3/_2$, and $S_2 = 1$ without a correction for monomeric paramagnetic impurity and TIP = 0 we obtained a reasonable fit with $J = -150$ cm^{-1} and $g = 1.89$.

Table VI. Cyclic Voltammetry of (**1**)$(PF_6)_3$ in Aqueous Solution at 22 °C[a] at an Au Electrode

pH	$E°$, V vs NHE	$I_{p,red}/I_{p,ox}$	ΔE_p, mV	cf(ox), μA V$^{-1/2}$ s$^{1/2}$ mmol^{-1} L	reversibility
11[b]	−0.091	0.64	85	44	qr
9[c]	−0.090	0.97	70	37	rev
8[d]	−0.073	0.87	75	42	rev
7[e]	−0.037	0.87	65	34	rev
6[f]	+0.017	0.80	85	27	rev
5[f]	+0.067	0.84	85	21	rev
4[g]	+0.120	0.97	85	31	rev
3.6[g]	+0.142	0.87	115	21	rev
3.2[g]	+0.14	0.48	160		irr
2.84[h]	+0.14	0.42	115		irr

[a] [(**1**)$(PF_6)_3$] = (4–7) × 10^{-4} M; scan rate of 50, 100, and 200 mV s^{-1}. Key: gr, quasi-reversible; rev, reversible; irr, irreversible. [b] Glycine/NaOH/NaCl buffer. [c] Boric acid/KCl/NaOH buffer. [d] Borax/HCl buffer. [e] KH_2PO_4/Na_2HPO_4 buffer. [f] Citric acid/NaOH buffer. [g] Sodium acetate/HAc buffer. [h] $LiClO_4/HClO_4$.

Electrochemistry. Figure 4 shows a cyclic voltammogram of a dried sample of (**2**)$(PF_6)_2$ in acetonitrile. Measurements over the range +0.5 to −2.2 V vs Ag/AgCl revealed two reversible one-electron waves at −0.49 V (ΔE_{pp} = 55 mV at a scan speed of 50 mV s^{-1}) and −2.31 V vs Fc^+/Fc (ΔE_{pp} = 65 mV at a scan rate of 50 mV s^{-1}). The peak current ratios I_{pa}/I_{pc} were found to be 1.0 ± 0.1 for both waves; they are independent of the scan rate (50–200 mV s^{-1}). Controlled-potential coulometry at −0.3 and −2.5 V vs Fc^+/Fc revealed a one-electron oxidation and a one-electron reduction of **2**, respectively. Thus the mixed-valence $Mo^{III}Mo^{IV}$ and $Mo^{II}Mo^{III}$ species are generated electrochemically in an aprotic solvent as in eq 4 and 5. The comproportionation

$$[L_2Mo^{III}_2(\mu\text{-}O)(\mu\text{-}CH_3CO_2)_2]^{2+} \overset{E_1}{\rightleftharpoons} [L_2Mo^{III}Mo^{IV}(\mu\text{-}O)(\mu\text{-}CH_3CO_2)_2]^{3+} + e^- \quad (4)$$

$$[L_2Mo^{III}_2(\mu\text{-}O)(\mu\text{-}CH_3CO_2)_2]^{2+} + e^- \overset{E_2}{\rightleftharpoons} [L_2Mo^{II}Mo^{III}(\mu\text{-}O)(\mu\text{-}CH_3CO_2)_2]^{+} \quad (5)$$

constant K_p, eq 6, is calculated to be 10^{70} at 25 °C from the

$$[Mo^{III}Mo^{IV}]^{3+} + [Mo^{II}Mo^{III}]^{+} \overset{K_p}{\rightleftharpoons} 2[Mo^{III}_2]^{2+} \quad (6)$$

difference of the redox potentials ($E_1 - E_2$). Oxidation of **2** by oxygen yields **3**, which has been isolated as a PF_6 salt (see above). It has not been possible to isolate the $Mo^{II}Mo^{III}$ mixed-valence species. The CV of (**3**)$(PF_6)_3$ measured in acetonitrile is identical with the one described above for **2**.

The cyclic voltammogram of (**1**)$(PF_6)_3$ in aqueous solution at an Au working electrode in the potential range −0.5 to +0.5 V vs Ag/AgCl reveals one reversible one-electron wave at pH > 3.0. If the pH is lower than 3, this wave becomes irreversible. We have therefore studied the pH dependence of the reversible wave, which corresponds to the oxidation of the Mo^{III}_2 dimer to the $Mo^{III}Mo^{IV}$ mixed-valence species, in the pH range 3–11. The

(27) Brorson, M.; Schäffer, C. E. *Acta Chem. Scand., Ser. A* **1986**, *40*, 358.
(28) O'Connor, C. J. *Prog. Inorg. Chem.* **1982**, *29*, 203.
(29) Chaudhuri, P.; Winter, M.; Küppers, H.-J.; Wieghardt, K.; Nuber, B.; Weiss, J. *Inorg. Chem.* **1987**, *26*, 3302.
(30) (a) Stranger, R.; Grey, I. E.; Madsen, I. C.; Smith, P. W. *J. Solid State Chem.* **1987**, *69*, 162. (b) Grey, I. E.; Smith, P. W. *Aust. J. Chem.* **1971**, *24*, 73. (c) Saillant, R.; Jackson, R. B.; Streib, W. E.; Folting, K.; Wentworth, R. A. D. *Inorg. Chem.* **1971**, *10*, 1453.

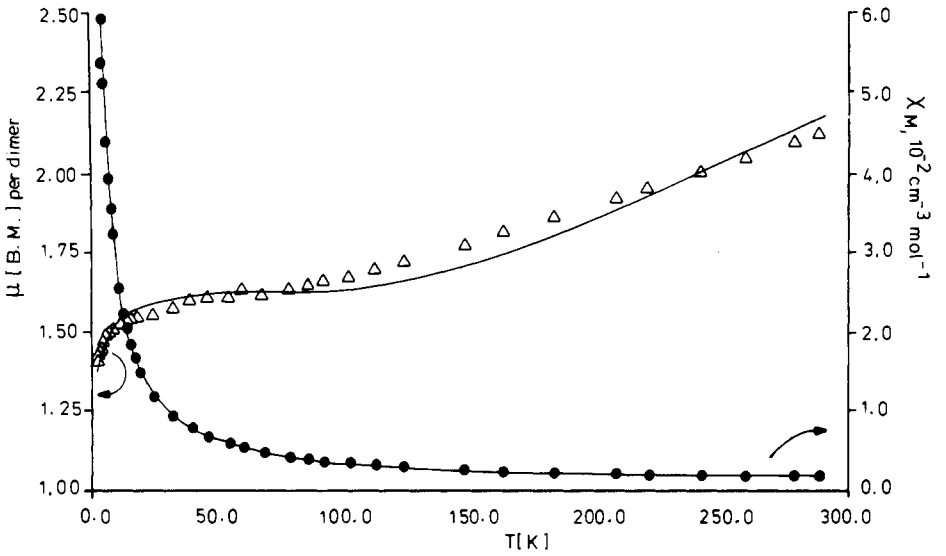

Figure 3. Plot of χ_M (or μ_{eff}) of $(3)(ClO_4)_3 \cdot H_2O$ versus the temperature (● and △ are experimental data; solid lines represent a best fit).

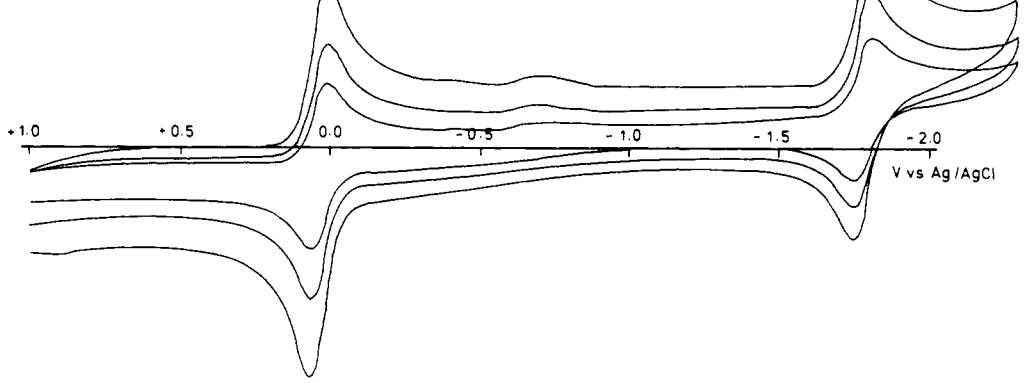

Figure 4. Cyclic voltammogram of $(2)(PF_6)_2$ in 0.1 M $(TBA)PF_6$ acetonitrile at 20 °C (glassy-carbon working electrode; scan rates of 50, 100, and 200 mV s^{-1}).

redox potential was found to shift to more positive potentials as the pH decreases from 8 to 4. In the pH range 9–11, the redox potential remains constant at –0.09 V vs NHE (Table VI). In the latter pH range the fully deprotonated species **2** is reversibly oxidized to **3** (eq 8). A plot of the measured redox potential vs

$$\mathbf{1} \overset{K_a}{\rightleftharpoons} \mathbf{2} + H^+ \qquad (7)$$

$$\mathbf{2} \overset{E_1}{\rightleftharpoons} \mathbf{3} + e^- \qquad (8)$$

pH is shown in Figure 5. The gradient of –0.053 V/pH indicates near-Nernstian behavior (0.059 V/pH) for a one-electron-, one-proton-transfer process (eq 7 and 8). The experimental pK_a value evaluated from this plot is 7.8 ± 0.2 in agreement with the spectrophotometrically determined value of 7.3 ± 0.2.

It is interesting that the μ-hydroxo-bridged complex **1** cannot be reversibly oxidized to form a protonated species of **3**. Considering the accompanying structural changes on going from **1** to **2** and **3** where the former species (**1**) has no Mo–Mo bonding interaction and the latter two species (**2** and **3**) do have Mo–Mo bonds, it appears that an electron may be reversibly removed from or added to suitable low-lying metal–metal molecular orbitals in **2**, but in the case of **1** its oxidation would be centered at one molybdenum ion to form a Mo(IV) center and the resulting hydroxo-bridged $Mo^{III}Mo^{IV}$ dimer containing a genuine Mo(III) center and a Mo(IV) center may not be stable in aqueous solution.

Description of Crystal Structures. The structure of the cation in $(1)(ClO_4)_3 \cdot H_2O$, shown in Figure 6, consists of two molybdenum atoms bridged by hydroxide and two acetate groups with two

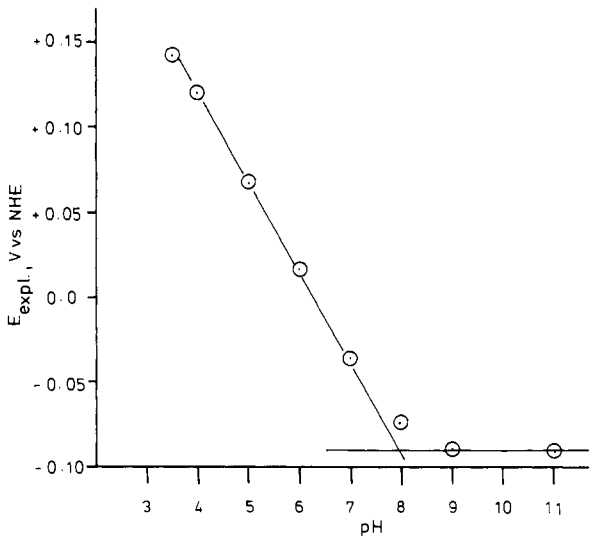

Figure 5. pH dependence of the redox potential of the couple $[L_2Mo_2(\mu\text{-}O)(\mu\text{-}CH_3CO_2)_2]^{3+/2+}$ (Au working electrode).

capping tridentate 1,4,7-trimethyl-1,4,7-triazacyclononane ligands. Table VII gives important bond lengths and angles. The H atom position of the OH bridge was not located in a difference Fourier map; the $Mo\text{–}O_{hydroxo}$ distance of 2.09 Å is characteristic for molybdenum(III) dimers with bridging hydroxo groups.[31,32] Each

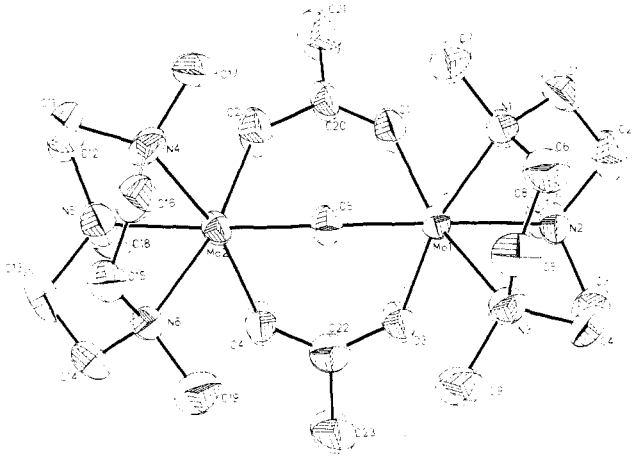

Figure 6. Structure of the trication in $(1)(ClO_4)_3 \cdot H_2O$ and atom-labeling scheme.

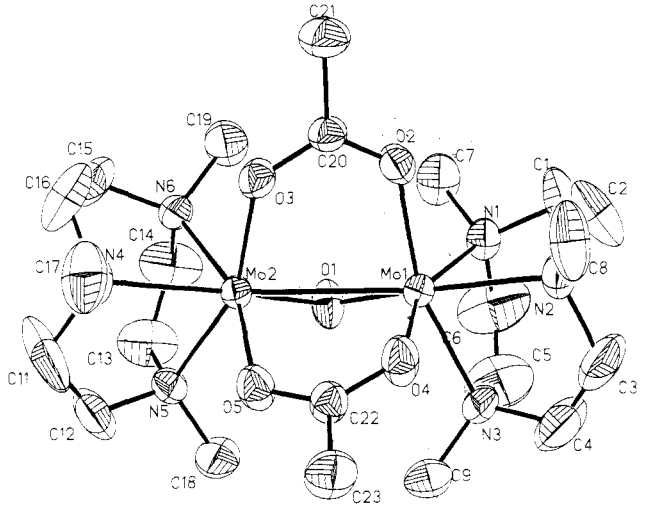

Figure 7. Structure of the dication in $(2)(BF_4)(ClO_4) \cdot H_2O$ and atom-labeling scheme.

Table VII. Selected Bond Lengths (Å) and Angles (deg) in $(1)(ClO_4)_3 \cdot H_2O$

O(3)-C(22)	1.250 (13)		
Mo(1)-N(1)	2.198 (9)	Mo(1)-N(2)	2.205 (8)
Mo(1)-N(3)	2.194 (9)	Mo(1)-O(1)	2.100 (7)
Mo(1)-O(3)	2.082 (7)	Mo(1)-O(5)	2.098 (7)
Mo(2)-N(5)	2.189 (10)	Mo(2)-N(4)	2.177 (9)
Mo(2)-O(2)	2.092 (7)	Mo(2)-N(6)	2.214 (9)
Mo(2)-O(5)	2.107 (7)	Mo(2)-O(4)	2.075 (7)
Mo(1)-Mo(2)	3.555 (1)	O(1)-C(20)	1.214 (13)
O(4)-C(22)	1.249 (13)	O(2)-C(20)	1.290 (12)
N(1)-Mo(1)-N(2)	81.1 (3)	N(1)-Mo(1)-N(3)	80.9 (3)
N(2)-Mo(1)-N(3)	80.2 (3)	N(1)-Mo(1)-O(1)	91.3 (3)
N(2)-Mo(1)-O(1)	90.6 (3)	N(3)-Mo(1)-O(1)	168.7 (3)
N(1)-Mo(1)-O(3)	167.6 (3)	N(2)-Mo(1)-O(3)	88.2 (3)
N(3)-Mo(1)-O(3)	91.3 (3)	O(1)-Mo(1)-O(3)	94.9 (3)
N(1)-Mo(1)-O(5)	98.1 (3)	N(2)-Mo(1)-O(5)	176.7 (3)
N(3)-Mo(1)-O(5)	96.6 (3)	O(1)-Mo(1)-O(5)	92.6 (3)
O(3)-Mo(1)-O(5)	92.3 (3)		
N(4)-Mo(2)-N(6)	80.8 (4)	N(5)-Mo(2)-N(6)	81.0 (4)
N(4)-Mo(2)-O(2)	94.4 (3)	N(5)-Mo(2)-O(2)	86.2 (3)
N(6)-Mo(2)-O(2)	166.9 (3)	N(4)-Mo(2)-O(4)	167.6 (3)
N(5)-Mo(2)-O(4)	91.8 (3)	N(6)-Mo(2)-O(4)	88.6 (3)
O(2)-Mo(2)-O(4)	94.7 (3)	N(4)-Mo(2)-O(5)	95.9 (3)
N(5)-Mo(2)-O(5)	176.3 (3)	N(6)-Mo(2)-O(5)	99.1 (3)
O(2)-Mo(2)-O(5)	93.5 (3)	O(4)-Mo(2)-O(5)	92.0 (3)
C(20)-O(1)-Mo(1)	139.9 (7)	Mo(2)-O(2)-C(20)	136.1 (7)
C(22)-O(3)-Mo(1)	135.0 (7)	Mo(2)-O(4)-C(22)	136.7 (7)

molybdenum(III) center is in distorted octahedral environment (*fac*-N_3O_3 donor set), and the Mo–O and Mo–N bond distances

Table VIII. Selected Bond Lengths (Å) and Angles (deg) in $(2)(BF_4)(ClO_4) \cdot 2H_2O$

Mo(1)-O(1)	1.945 (4)	Mo(1)-O(2)	2.102 (4)
Mo(1)-O(4)	2.097 (4)	Mo(1)-N(1)	2.260 (4)
Mo(1)-N(2)	2.291 (5)	Mo(1)-N(3)	2.243 (7)
Mo(1)-Mo(2)	2.885 (1)	Mo(2)-O(3)	2.100 (4)
Mo(2)-O(1)	1.946 (4)	Mo(2)-N(6)	2.257 (5)
Mo(2)-O(5)	2.085 (4)	O(2)-C(20)	1.242 (8)
Mo(2)-N(5)	2.252 (4)	C(20)-O(3)	1.256 (5)
Mo(2)-N(4)	2.298 (6)	O(4)-C(22)	1.263 (6)
		C(22)-O(5)	1.260 (7)
O(1)-Mo(1)-O(2)	102.3 (2)	O(1)-Mo(1)-O(4)	112.0 (1)
O(2)-Mo(1)-O(4)	96.3 (2)	O(1)-Mo(1)-N(1)	85.8 (2)
O(2)-Mo(1)-N(1)	91.7 (2)	O(4)-Mo(1)-N(1)	158.2 (2)
O(1)-Mo(1)-N(2)	161.5 (2)	O(2)-Mo(1)-N(2)	86.3 (2)
O(4)-Mo(1)-N(2)	82.8 (1)	N(1)-Mo(1)-N(2)	77.5 (2)
O(1)-Mo(1)-N(3)	91.2 (2)	O(2)-Mo(1)-N(3)	162.9 (1)
O(4)-Mo(1)-N(3)	88.0 (2)	N(1)-Mo(1)-N(3)	78.9 (2)
N(2)-Mo(1)-N(3)	77.8 (2)	Mo(1)-Mo(2)-O(1)	42.1 (1)
O(2)-Mo(1)-Mo(2)	80.2 (1)	O(1)-Mo(2)-O(3)	108.6 (1)
Mo(1)-O(1)-Mo(2)	95.7 (2)	O(1)-Mo(2)-O(5)	106.0 (2)
Mo(1)-Mo(2)-O(3)	79.4 (1)	Mo(1)-Mo(2)N(4)	156.1 (1)
Mo(1)-Mo(2)-O(5)	80.4 (1)	O(3)-Mo(2)-N(4)	83.0 (2)
O(3)-Mo(2)-O(5)	97.1 (2)	Mo(1)-Mo(2)-N(5)	121.2 (2)
O(1)-Mo(2)-N(4)	161.7 (2)	O(3)-Mo(2)-N(5)	159.1 (2)
O(5)-Mo(2)-N(4)	85.9 (2)	N(4)-Mo(2)-N(5)	78.1 (2)
O(1)-Mo(2)-N(5)	87.8 (2)	O(1)-Mo(2)-N(6)	88.8 (2)
O(5)-Mo(2)-N(5)	90.4 (2)	O(5)-Mo(2)-N(6)	161.5 (1)
Mo(1)-Mo(2)-N(6)	118.0 (1)	N(5)-Mo(2)-N(6)	78.9 (2)
O(3)-Mo(2)-N(6)	88.3 (2)		
N(4)-Mo(2)-N(6)	77.2 (2)		

Table IX. Selected Bond Lengths (Å) and Angles (deg) in $(3)(ClO_4)_3 \cdot H_2O$

Mo(1)-N(1)	2.220 (7)	Mo(1)-N(2)	2.199 (6)
Mo(1)-N(3)	2.278 (9)	Mo(1)-Mo(2)	2.969 (1)
Mo(1)-O(1)	2.049 (7)	Mo(1)-O(3)	2.053 (5)
Mo(1)-O(5)	1.901 (7)	Mo(2)-N(4)	2.235 (10)
Mo(2)-N(5)	2.215 (9)	Mo(2)-N(6)	2.197 (8)
Mo(2)-O(2)	2.049 (6)	Mo(2)-O(4)	2.043 (6)
Mo(2)-O(5)	1.939 (9)	O(1)-C(21)	1.267 (14)
O(2)-C(21)	1.251 (12)	O(4)-C(23)	1.259 (14)
O(3)-C(23)	1.272 (12)		
N(1)-Mo(1)-N(2)	79.3 (3)	N(1)-Mo(1)-N(3)	77.9 (3)
N(2)-Mo(1)-N(3)	78.7 (3)	N(2)-Mo(1)-O(1)	87.8 (3)
N(1)-Mo(1)-O(1)	158.6 (3)	N(2)-Mo(1)-O(3)	159.7 (3)
N(3)-Mo(1)-O(1)	83.0 (3)	N(1)-Mo(1)-O(5)	86.5 (4)
N(1)-Mo(1)-O(3)	89.9 (3)	N(3)-Mo(1)-O(5)	164.4 (4)
N(3)-Mo(1)-O(3)	82.2 (2)	O(1)-Mo(1)-O(5)	112.6 (3)
O(1)-Mo(1)-O(3)	96.9 (2)	N(4)-Mo(2-N(5)	78.7 (4)
N(2)-Mo(1)-O(5)	99.5 (3)	N(4)-Mo(2)-N(6)	78.7 (3)
O(3)-Mo(1)-O(5)	96.9 (3)	N(5)-Mo(2)-O(2)	160.6 (4)
N(5)-Mo(2)-N(6)	79.7 (3)	N(5)-Mo(2)-O(4)	86.8 (3)
N(4)-Mo(2)-O(2)	83.1 (3)	O(2)-Mo(2)-O(4)	98.1 (3)
N(6)-Mo(2)-O(2)	90.4 (3)	N(4)-Mo(2)-O(5)	166.1 (3)
N(4)-Mo(2)-O(4)	84.6 (3)	N(6)-Mo(2)-O(5)	96.3 (3)
N(6)-Mo(2)-O(4)	160.2 (3)	O(4)-Mo(2)-O(5)	97.5 (3)
N(5)-Mo(2)-O(5)	87.7 (3)		
O(2)-Mo(2)-O(5)	110.1 (3)		
Mo(1)-O(5)-Mo(2)	101.3 (3)		

of both Mo(III) ions are within experimental error identical. The Mo–N lengths are equivalent (mean 2.196 Å); no structural trans influence of the hydroxo bridge is observed. The Mo···Mo distance of 3.555 (1) Å rules out a significant attractive interaction between the molybdenum atoms; **1** is a classical complex of the Werner-type. The structure resembles in this respect first-row transition-metal complexes that contain the (μ-hydroxo)bis(μ-acetato)dimetal core[29] and Walton's oxo-bridged osmium(IV) dimer[24] where M···M distances >3.1 Å have been observed. It

(31) (a) Kneale, G. G.; Geddes, A. J.; Sasaki, Y.; Shibahara, T.; Sykes, A. G. *J. Chem. Soc., Chem. Commun.* **1975**, 356. (b) Kneale, G. G.; Geddes, A. J. *Acta Crystallogr., Sect. B* **1975**, *B31*, 1233.
(32) Wieghardt, K.; Hahn, W.; Swiridoff, W.; Weiss, J. *Inorg. Chem.* **1984**, *23*, 94.

Table X. Comparison of Structures[a]

	1	2	3	$[([9]aneN_3)_2Mo_2^{III}(\mu\text{-}OH)_2(\mu\text{-}CH_3CO_2)]\text{-}I_3\cdot H_2O$
$M-O_{oxo/hydroxo}$, Å	2.090	1.945	1.920	2.076
$M-O_{acetate}$, Å	2.087	2.096	2.048_5	2.086
$M-N_{trans}$,[b] Å	2.197	2.294_5	2.256_5	2.216
$M-N_{cis}$,[c] Å	2.196	2.253	2.208	2.209
Mo–O–Mo, deg	115.4 (3)	95.7 (2)	101.3 (3)	73.0
Mo···Mo, Å	3.555 (1)	2.885 (1)	2.969 (1)	2.471
trans influence,[d] Å	0.001	0.042	0.048	0.007

[a] Average bond distances. [b] Mo–N bond distance trans to the $M-O_{oxo/hydroxo}$ bond. [c] Mo–N bonds cis to the $M-O_{oxo/hydroxo}$ bond. [d] Difference between $M-N_{trans}$ and $M-N_{cis}$ bond lengths.

is noted that complexes containing the (μ-acetato)bis(μ-hydroxo)dimolybdenum(III) core are green and diamagnetic; the Mo–Mo distance of 2.47 Å is indicative of a Mo–Mo triple bond ($\sigma^2\pi^2\delta^2$).[31,32] **1** represents the first structurally characterized classical Mo(III) dimer without metal–metal bonding. The structure of the dication in **(2)**$(BF_4)(ClO_4)\cdot H_2O$, shown in Figure 7, is very similar to that of **1** with three significant exceptions (Table VIII). (i) The $Mo-O_{oxo}$ bond distances are shorter by 0.145 Å than the $Mo-O_{hydroxo}$ bonds in **1** (Table VIII and X). (ii) The Mo–Mo distance of 2.885 (1) Å is shorter by 0.67 Å(!!). It is the shortest metal–metal distance observed in (μ-oxo)bis(μ-acetato)dimetal complexes to date. (iii) The Mo–N bonds in the trans position relative to the μ-oxo bridge are significantly longer (by 0.042 Å) than those in the trans positions relative to $Mo-O_{acetate}$ bonds. Thus a structural trans influence is observed in **2**. The $Mo-N_{cis}$ and $Mo-O_{acetate}$ bond distances in **1** and **2** are identical within experimental error.

Is the Mo–Mo distance of 2.885 (1) Å in **2** indicative of a bonding interaction between the molybdenum atoms, or does it simply reflect a forced approach of these metal atoms induced by the contraction of the $Mo-O_b$ bond on going from a hydroxo bridge in **1** to an oxo bridge in **2**? A comparison with Lippard's two diiron(III) complexes is very instructive.[20,33] Both the hydroxo-bridged complex $[(HB(pz)_3)Fe(\mu\text{-}OH)(\mu\text{-}CH_3CO_2)_2Fe(HB(pz)_3)]^+$ (A) and its deprotonated analogue $[(HB(pz)_3)Fe(\mu\text{-}O)(\mu\text{-}CH_3CO_2)_2Fe(HB(pz)_3)]$ (B) have been characterized by X-ray crystallography. The Fe···Fe distances are 3.439 (1) Å in A and 3.146 (1) Å in B; the mean Fe–O bond lengths are 1.956 Å in A and 1.784 (2) Å in B. Thus a contraction of the Fe–O bonds by 0.17 Å, which is more pronounced than in **1** and **2**, leads to a closer approach of the iron atoms by only 0.29 Å, which is to be compared with 0.67 Å in **1** and **2**. Therefore, we conclude by considering here only the structural features of **1** and **2** that an attractive interaction exists between the molybdenum(III) atoms in **2**. In addition it is noted, that only complex B exhibits a trans influence on the Fe–N bonds trans to the $Fe-O_{oxo}$ bonds and not A—just as is the case in **2** and **1**.

The structure of the trication is **(3)**$(ClO_4)_3\cdot H_2O$ is shown in Figure 8; Table IX gives bond lengths and angles. The structure of **3** is very similar to that of the dication **2**. The oxidation of **2** to **3** by one electron leads to a small contraction of all Mo–N and Mo–O bonds as compared to those in **2**. Thus $Mo-N_{trans}$ and $Mo-N_{cis}$ are shorter by 0.038 and 0.045 Å, as are $Mo-O_{oxo}$ and $Mo-O_{acetate}$ bonds by 0.025 and 0.048 Å, respectively. *It is only the Mo–Mo distance that increases by 0.084 Å despite the fact that all other bond lengths decrease on going from* **2** *to* **3**. Clearly, a strong trans influence of the oxo bridge is also observed in **3** (Table X). The $Mo-O_{oxo}$ bond distance of 1.92 Å agrees well with values of 1.90 and 1.93 Å found in the mixed-valence $Mo^{III}_2Mo^{IV}_2$ tetramer $Na_4[Mo_4O_4(OH)_2(edta)_2]\cdot 12H_2O$.[34] As a consequence of the increased Mo–Mo distance in **3** the Mo–O–Mo bond angle increases by 5.6°.

In Walton's neutral, diamagnetic osmium(IV) dimer (d^4–d^4) the Os···Os distance is 3.440 (2) Å; the authors have left open

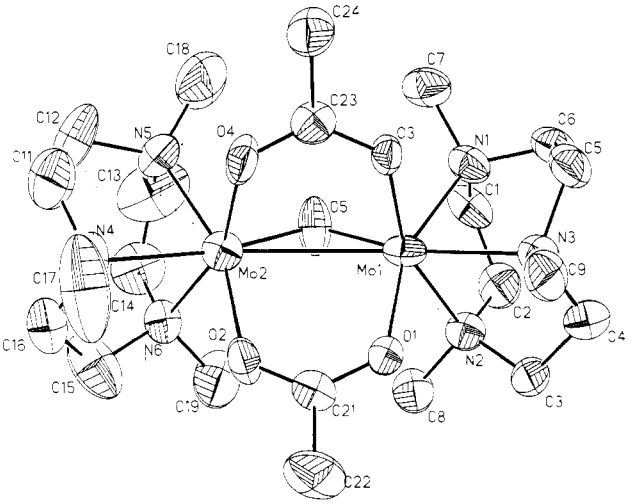

Figure 8. Structure of the trication in **(3)**$(ClO_4)_3\cdot H_2O$ and atom-labeling scheme.

Scheme I

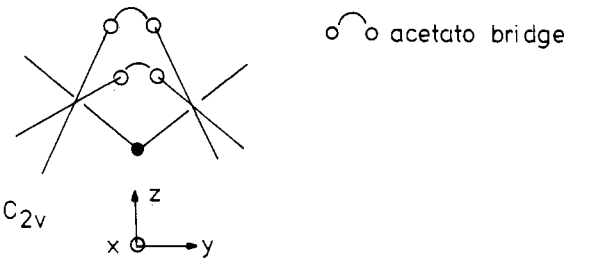

the question as to whether or not a bonding interaction between the osmium atoms exists.[24] In the light of the Mo–Mo distances in **2** and **3**, we feel that most probably no such interaction exists in this case (the effective ionic radii of 6-coordinate Os(IV) and Mo(III) or Mo(IV) are very similar (~0.65 Å)).[35]

The observed Mo–O and Mo–N contractions in **3** are due to the increased positive charge of the dimer by one unit as compared to **2**. The Mo–Mo bond lengthening clearly indicates that the removed electron stems from a predominantly bonding metal–metal molecular orbital.

Thus the structural features of **1**–**3** give a consistent picture, assuming an attractive interaction between the molybdenum atoms in **2** and **3** but not in **1**.

Metal–Metal Bonding in 2 and 3. **2** and **3** may be viewed to a first approximation as cofacial bioctahedral complexes where the ideal D_{3h} symmetry of a hypothetical $[LMo(\mu\text{-}X)_3MoL]^{3+}$ complex (X = Cl, Br, or OH) is lowered to effective C_{2v} by substituting two μ-X by two symmetrical μ-acetato bridges. The most lucid axes of quantization for the two metal atoms are defined as in Scheme I. With this choice of axes the orbitals of interest

(33) Armstrong, W. H.; Lippard, S. J. *J. Am. Chem. Soc.* **1984**, *106*, 4632.
(34) Shibahara, T.; Sheldrick, B.; Sykes, A. G. *J. Chem. Soc., Chem. Commun.* **1976**, 523.
(35) Shannon, R. D.; Prewitt, C. T. *Acta Crystallogr., Sect. B* **1970**, *B26*, 1076.

for metal-metal bonding will be those not involved in metal-ligand σ-bonding (d_{xz}, d_{yz}, d_{xy} orbitals on the metal atom). From the analyses of McCarley et al.,[36] Hoffmann et al.,[37] Wentworth et al.,[38] and Cotton et al.[39] there are three bonding molecular orbitals in D_{3h} symmetry ($a_1' < e' < e'' < a_2''$), where the $\sigma(a_1')$ and $\pi(e')$ orbitals are bonding and the $\pi(e'')$ and $\pi(a_2'')$ orbitals are antibonding. The descent in symmetry to C_{2v} converts them to the following representations: $a'(\sigma) \rightarrow a_1$, $a_2''(\sigma^*) \rightarrow b_2$, $e'(\pi_1) \rightarrow a_1$, $e'(\pi_2) \rightarrow b_1$, $e''(\pi_3^*) \rightarrow b_2$, and $e''(\pi_4^*) \rightarrow a_2$. The a_1 MO remains a σ bond of the lowest energy of the set, which is occupied with two electrons, whereas the $a_1(\pi)$ and $b_1(\pi)$ orbitals are occupied by the remaining four electrons. Thus the formal metal-metal bond order in **2** is 3 ($\sigma^2\pi^4$). Note, the two π orbitals are not degenerate in C_{2v}. Again from McCarley's argumentation, the b_1 π orbital may be lower in energy than the $a_1\pi$ orbital and the ground state in **2** may be described as $[\sigma(a_1)]^2[\pi(b_1)]^2[\pi(a_1)]^2$ and the observed two low-energy transitions in the electronic spectrum of (**2**) (Figure 1) may be assigned to allowed $\pi(a_1) \rightarrow \pi^*(a_1)$ and $\pi(a_1) \rightarrow \pi^*(b_1)$. In **3** the ground state then is $[\sigma(a_1)]^2[\pi(b_1)]^2[\pi(a_1)]^1$; one electron of **2** is removed from a bonding metal-metal MO, and consequently, the Mo-Mo bond in **3** is longer than that in **2** and the bond order is 2.5. The electrochemically generated mixed-valence $Mo^{II}Mo^{III}$ species would have to accommodate the additional electron in an antibonding metal-metal $\pi^*(a_1)$ orbital, and also an increase of the Mo-Mo bond is expected (the bond order is again 2.5).

Conclusion

We have shown in this study that the classical Werner-type complex **1** is reversibly transformed by deprotonation at the bridging hydroxo group into a metal-metal-bonded (μ-oxo)bis(μ-acetato)dimolybdenum(III) species (bond order 3). This intramolecular base-induced Mo-Mo bond formation is unprecedented and is believed to be a consequence of the substantial Mo-O bond contraction on going from a μ-hydroxo to an μ-oxo bridge, which brings the Mo(III) centers in close enough proximity to induce an overlap of the metal d_{xy}, d_{xz}, d_{yz} orbitals to form a weak Mo-Mo triple bond ($\sigma^2\pi^4$). This observation is nicely corroborated by the ease of a one-electron oxidation of **2** to produce **3** with a slightly longer Mo-Mo bond of order 2.5 ($\sigma^2\pi^3$).

Acknowledgment. We thank the Fonds der Chemischen Industrie for financial support of this work. A.N. is grateful to CNPq (Brazil) for a stipend during 1987. We thank Prof. W. Haase and Dipl.-Ing. S. Gehring (Universität Darmstadt) for measurements of temperature-dependent magnetic susceptibilities.

Registry No. **1**$(PF_6)_3$, 114198-91-3; **1**$(ClO_4)_3 \cdot H_2O$, 114198-93-5; **2**$(PF_6)_2 \cdot 3H_2O$, 118335-23-2; **2**$(ClO_4)(BF_4) \cdot H_2O$, 114198-97-9; **3**$(PF_6)_3$, 118335-25-4; **3**$(ClO_4)_3 \cdot H_2O$, 118335-27-6; $LMoBr_3$, 94370-80-6; $[L_2Mo^{II}Mo^{III}(\mu\text{-}O)(\mu\text{-}CH_3CO_2)_2]^+$, 118335-28-7; Mo, 7439-98-7.

Supplementary Material Available: Tables listing bond lengths (Tables SI-SIII), bond angles (Tables SIV-SVI), derived hydrogen positions (Tables SVII-SIX), and anisotropic temperature factors (Tables SX-SXII) and a full table of crystal data (Table SXIII) for structures **1-3**, respectively (14 pages); tables of calculated and observed structure factors (94 pages). Ordering information is given on any current masthead page.

(36) Templeton, J. L.; Dorman, W. C.; Clardy, J. C.; McCarley, R. E. *Inorg. Chem.* **1978**, *17*, 1263.
(37) Summerville, R. H.; Hoffmann, R. *J. Am. Chem. Soc.* **1979**, *101*, 3821.
(38) Saillant, R.; Wentworth, R. A. D. *J. Am. Chem. Soc.* **1969**, *91*, 2174.
(39) (a) Cotton, F. A.; Ucko, D. A. *Inorg. Chim. Acta* **1972**, *6*, 161. (b) Cotton, F. A. *Pure Appl. Chem.* **1967**, *17*, 25.
(40) Cotton, F. A.; Diebold, M. P.; O'Connor, C. J.; Powell, G. L. *J. Am. Chem. Soc.* **1985**, *107*, 7438.

Contribution from the Department of Chemistry, Colorado State University, Fort Collins, Colorado 80523

Five- and Six-Coordinate High-Spin Iron(III) Porphyrin Complexes with Teflate ($OTeF_5^-$) Ligands

Patti J. Kellett,[‡] Michael J. Pawlik, Lucille F. Taylor, Ronald G. Thompson, Mark A. Levstik, Oren P. Anderson, and Steven H. Strauss*,[1]

Received June 14, 1988

The compounds Fe(TPP)($OTeF_5$) and Fe(OEP)($OTeF_5$), together with their ^{18}O analogues, were prepared and characterized by using magnetic susceptibility measurements and ^1H and ^{19}F NMR, UV-vis, and mid- and far-infrared spectroscopy. The solution behavior of Fe(TPP)($OTeF_5$) was investigated by cyclic voltammetry and ligand replacement reactions. The data indicate that these complexes contain high-spin iron(III) and that the relative ligand field strength of the $OTeF_5^-$ anion follows the order $Cl^- > OTeF_5^- > ClO_4^-$. The compound Fe(TPP)($OTeF_5$)(THF) was examined by single-crystal X-ray diffraction. This compound crystallized in the triclinic system, space group $P\bar{1}$ ($Z = 1$), with $a = 9.524$ (3) Å, $b = 11.069$ (2) Å, $c = 11.843$ (3) Å, $\alpha = 102.64$ (2)°, $\beta = 104.45$ (2)°, and $\gamma = 114.44$ (2)°. The $OTeF_5^-$ and THF ligands were disordered; the best model placed the $OTeF_5^-$ ligand above the porphyrin plane 65% of the time. The Fe-N_p distances of 2.064 (5), 2.011 (5), 2.047 (5), and 2.086 (4) Å are indicative of high-spin ($S = {}^5/_2$) iron(III). The iron atom is displaced toward the $OTeF_5^-$ ligand by 0.20 Å, the Fe-O($OTeF_5$) distance is 1.967 (5) Å, and Fe-O(THF) is 2.334 (7) Å. This is only the second structurally characterized six-coordinate high-spin iron(III) porphyrin complex with different axial ligands.

Introduction

Despite the well-developed use of pentafluoroorthotellurate ($OTeF_5$) as a bulky and electronegative substituent for main-group elements (e.g. $Xe(OTeF_5)_2$,[2] $B(OTeF_5)_3$,[3] $I(OTeF_5)_5$[4]),[5] the chemistry of $OTeF_5^-$ (teflate) as a ligand for transition metals, especially in oxidation states ≤ 3, has only recently been explored.[6,7] One of our goals is to make use of any unique electronic, steric, and structural properties of teflate to modify the chemical properties of metal ions in new ways. If this is to be done in a rational way, the properties of teflate as a ligand must be fully

[‡] Formerly Patti K. Miller.

(1) Alfred P. Sloan Fellow, 1987-1989.
(2) Sladky, F. *Monatsh. Chem.* **1970**, *101*, 1559.
(3) (a) Kropshofer, H.; Leitzke, O.; Peringer, P.; Sladky, F. *Chem. Ber.* **1981**, *114*, 2644. (b) Sawyer, J. F.; Schrobilgen, G. J. *Acta Crystallogr., Sect. B: Struct. Crystallogr. Cryst. Chem.* **1982**, *B38*, 1561.
(4) Seppelt, K.; Lentz, D. *Z. Anorg. Allg. Chem.* **1980**, *460*, 5.
(5) (a) Seppelt, K. *Angew. Chem., Int. Ed. Engl.* **1982**, *21*, 877. (b) Engelbrecht, A.; Sladky, F. *Adv. Inorg. Chem. Radiochem.* **1981**, *24*, 189. (c) Seppelt, K. *Acc. Chem. Res.* **1979**, *12*, 211.

0020-1669/89/1328-0440$01.50/0